SLAC-PUB-7179
June 1996

RESONANCE BASIS MAPS AND nPB TRACKING FOR DYNAMIC APERTURE STUDIES *†

Y.T. Yan, J. Irwin, and T. Chen

Stanford Linear Accelerator Center, P.O. Box 4349, Stanford, CA 94309

In this article we outline the procedures we used for dynamic aperture studies of the PEP-II lattices with resonance basis maps and nPB tracking.

1 INTRODUCTION

Lie Algebraic methods[1] implemented with truncated power series algebra packages[2] or libraries,[3] have become important in nonlinear single-particle dynamics studies.[4] Algorithms for nonlinear normal forms[5] and one-turn map tracking, such as kick factorization[6] and integrable polynomial factorization,[7] have been becoming common numerical practices. Much progress has been made in the one-turn map tracking during the last decade — formerly regarded as "impossible" to a first successful demonstration[8] and then to a more thorough exploration for the kick factorization[9] and the implicit map.[10] In this article, we outline procedures used for PEP-II electron ring lattice studies using recently developed resonance basis maps[11] and nPB tracking .[12]

2 EXTRACTION OF A ONE-TURN TAYLOR MAP

The first step for leading to a resonance basis map is to extract a one-turn (or one-particular-module) Taylor map.

In a particle tracking code, given the initial phase-space coordinates (numbers) with respect to the closed orbit at a well chosen observation point in the lattice, one can advance the particle's coordinates element-by-element for a beam line or one turn (or more turns) to get a new set of coordinates (new numbers). Similarly, if one links the tracking code to a truncated power series algebra library, such as Zlib,[3] and properly replaces the statements of the tracking code to their corresponding truncated power series algebra statements and initializes the particle coordinates as the identity power series, one can then advance the coefficients of these power series

* Work supported by the Department of Energy under Contract No. DE-AC03-76SF00515

† presented at LHC 95 International Workshop on Single-particle Effects in Large Hadron Colliders, 15-21 October, 1995, Montreux, Switzerland; to appear in Particle Accelerators

element-by-element until one turn is reached to get a one-turn map truncated at a pre-set order. These power series are actually the final coordinates (after one turn) as functions, in Taylor series expansions, of the initial coordinates . In our common practice, we usually consider 2-dimensional maps with a parameter δ representing the momentum deviation dp/p. Thus, mathematically, the Taylor map can be expressed as

$$\vec{Z} = \vec{U}(\vec{z}, \delta) + \emptyset(N+1), \tag{1}$$

where $\emptyset(N+1)$ indicates that the Taylor map is truncated at an order of N, $\vec{z} = (x, p_x, y, p_y)$ is the global or initial phase-space coordinate vector and $\vec{Z} = (X, P_x, Y, P_y)$ is the phase-space coordinate vector after one turn. To include the synchrotron oscillation for a circular accelerator, we can additionally extract a time-of-flight Taylor map and then place an RF cavity at the end of the map.

3 SINGLE LIE TRANSFORMATION IN FLOQUET SPACE

Assuming that the Taylor map given by Eq. 1 is symplectic, as it should be since we would treat the radiation damping and quantum excitation globally with an externally inserted damped map, one can make a linear Floquet (Courant-Snyder) [13] transformation and then a single Lie transformation[1] to obtain

$$\vec{Z} = A^{-1}(\vec{z}, \delta) R(\vec{z}) e^{:f(\vec{z},\delta):} A(\vec{z}, \delta)\vec{z} + \emptyset'(N+1), \tag{2}$$

where $f(\vec{z}, \delta)$ is a polynomial from order 3 to order N + 1 and all nonlinear mapping is performed by the single Lie generator $e^{:f(\vec{z},\delta):}$; $R(\vec{z})$ is a one-turn pure rotational 4-by-4 matrix in the 4-dimensional transverse canonical phase-space, and $A(\vec{z}, \delta)$ and its inverse $A^{-1}(\vec{z}, \delta)$ are the 4-by-5 matrices that generate the Floquet transformation. The dispersion, η, and the Courant-Snyder parameters, α, β, and γ are all included in $A(\vec{z}, \delta)$ and $A^{-1}(\vec{z}, \delta)$. Thus, in the Floquet space the map is given by

$$M = R(\vec{z}) e^{:f(\vec{z},\delta):} \tag{3}$$

4 TRANSFORMATION TO ACTION-ANGLE VARIABLE SPACE

Just as the Cartesian coordinates x, p_x, y, p_y, the action-angle variables, $J_x, J_y, \theta_x, \theta_y$, along with the momentum deviation parameter, δ, can also form a complete base for the polynomial $f(\vec{z}, \delta)$ of the Lie transformation in Eq. 3. Through decomposition into a complete complex base consisting of the rotational eigen-modes

$$\hat{x}_\pm = x \mp i p_x = \sqrt{2J_x} e^{\pm i\theta_x}, \qquad \hat{y}_\pm = x \mp i p_y = \sqrt{2J_y} e^{\pm i\theta_y},$$

one can obtain

$$f(\vec{z},\delta) = f(J_x, J_y, \theta_x, \theta_y, \delta) =$$

$$\sum_{\vec{n}\vec{m}p} (2J_x)^{\frac{n_x}{2}} (2J_y)^{\frac{n_y}{2}} \delta^p [a_{\vec{n}\vec{m}p} cos(m_x\theta_x + m_y\theta_y) + b_{\vec{n}\vec{m}p} sin(m_x\theta_x + m_y\theta_y)], \quad (4)$$

where $\vec{n}$ and $\vec{m}$ are index vectors representing (n_x, n_y) and (m_x, m_y) respectively.

5 RESONANCE BASIS MAP

For convenience, we would separate the terms in Eq. 4 into two groups, one contains all those terms that are not angle variable dependent (tune shift terms), i.e. $m_x = m_y = 0$, and the other contains the rest of the terms (resonance driving terms) that all depend on angle variables. Then, after suitable factorization, the Floquet space map given by Eq. 3 can be written as

$$M = e^{:-h_T(J_x,J_y,\delta):} e^{:-h_R(\theta_x,J_x,\theta_y,J_y,\delta):}, \quad (5)$$

where

$$h_T(J_x, J_y, \delta) = \mu_x J_x + \mu_y J_y + \sum_{\vec{n},p} C_{\vec{n}p} (2J_x)^{\frac{n_x}{2}} (2J_y)^{\frac{n_y}{2}} \delta^p, \quad (6)$$

$$h_R(\theta_x, J_x, \theta_y, J_y, \delta) = \sum_{n_x+n_y+p=3}^{\Omega+1} \sum_{m_x=0}^{n_x} \sum_{m_y=-n_y}^{n_y} D_{\vec{n}\vec{m}p}(\theta_x, \theta_y) (2J_x)^{\frac{n_x}{2}} (2J_y)^{\frac{n_y}{2}} \delta^p, \quad (7)$$

and

$$D_{\vec{n}\vec{m}p}(\theta_x, \theta_y) = A_{\vec{n}\vec{m}p} cos(m_x\theta_x + m_y\theta_y) + B_{\vec{n}\vec{m}p} sin(m_x\theta_x + m_y\theta_y). \quad (8)$$

Note that in Eq. 6, the indices $\vec{n} = (n_x, n_y)$ are even numbers and we have represented $R(\vec{z})$ by its corresponding Lie form $e^{:-\mu_x J_x - \mu_y J_y:}$, where μ_x and μ_y are the working tunes of the lattice. Also note that each of the coefficients $C_{\vec{n}p}$ is the same as its corresponding coefficient $a_{\vec{n}\vec{m}p}$ with $m_x = m_y = 0$ in Eq. 4 while each of the coefficients $A_{\vec{n}\vec{m}p}$ or $B_{\vec{n}\vec{m}p}$ is generally different from its corresponding coefficient $a_{\vec{n}\vec{m}p}$ or $b_{\vec{n}\vec{m}p}$ in Eq. 4 due to factorization.

The physical picture of the Floquet space map represented by Eq. 5 is as follows: The first Lie transformation with its effective Hamiltonian represented by Eq. 6 performs an amplitude-dependent rotation and is followed by a nonlinear perturbation driven by the second Lie transformation with its effective Hamiltonian represented by Eq. 7. These are to be discussed in more detail in later sections.

6 THE GLOBAL LATTICE FILE

Once we obtain the resonance basis map given by Eq. 5, Eq. 6, and Eq. 7, we would usually write out these coefficients, $C_{\vec{n}p}, A_{\vec{n}\vec{m}p}$, and $B_{\vec{n}\vec{m}p}$ along with their

corresponding indices $\vec{n}, \vec{m}$, and p into a file. In the same file, we also write the 4-by-5 matrix A and its inverse A^{-1} that perform the linear Floquet transformation as shown in Eq. 2. We may also write, in the same file, the time-of-flight map, the linear radiation damping map, and related quantum excitation parameters. We would call this file the Global Lattice file. We can freely change the contents (usually a very limited key tune shift and/or resonance driving coefficients) and perform nPB tracking (to be described below) to obtain artificial dynamic apertures for probing the impact of these selected key terms on the dynamic aperture of the PEP-II lattices. In this way, we obtain clues toward better design for the real lattice.

7 THE nPB TRACKING

To efficiently evaluate the resonance basis maps given by Eq. 5, we use a newly developed method which directly performs Poisson bracket expansion of the resonance basis Lie generators to a suitable (n) order and so the name of nPB (n Poisson Bracket) tracking.[12] The Poisson brackets are evaluated using action-angle variables, but the resulting expressions are written as functions of the Cartesian coordinates. The Sines, Cosines, and square root that relate the Cartesian coordinates and the Polar (action-angle) coordinates need never be calculated and hence the fast speed.

To include the synchrotron oscillation and/or radiation damping and quantum excitation, one can always transform the particle phase-space Cartesian coordinates back and forth between the Floquet space and the real space with the Floquet transformation matrices A and A^{-1} given in Eq. 2. In the real space, with the inclusion of an accurate but concise time-of-flight map, we can insert a suitable RF cavity to update the momentum deviation parameter, δ for each turn of tracking. The updated momentum deviation parameter, δ, is then absorbed into the coefficients of the resonance basis map before direct Poisson expansion calculation of the resonance basis map. By the same token, radiation damping effects can also be included with the insertion of a suitable linear damping map and a suitable randomly generated excitation map.

8 REPLIABILITY AND SPEED OF THE nPB TRACKING

One may be concerned with the fact that the nPB tracking is not 100% accurate since the map is truncated at a moderate order and not 100% symplectic because one does not carry the Poisson bracket expansion to the infinite order. However, for the PEP-II lattice dynamic aperture studies, we only need to track particles for about 1000 turns since due to synchrotron radiation damping particles surviving for more than 1000 turns are very unlikely to get lost. From numerous tests we have concluded that a 10^{th}-order map with 3-Poisson-bracket expansion of the Lie transformation is accurate and symplectic enough for PEP-II lattice dynamic aperture studies. It takes about 1 minute with such a 10^{th}-order map, 3PB tracking

on a RISC workstation to obtain a dynamic aperture plot at a given working point, which would otherwise have taken a few hours with element-by-element tracking.

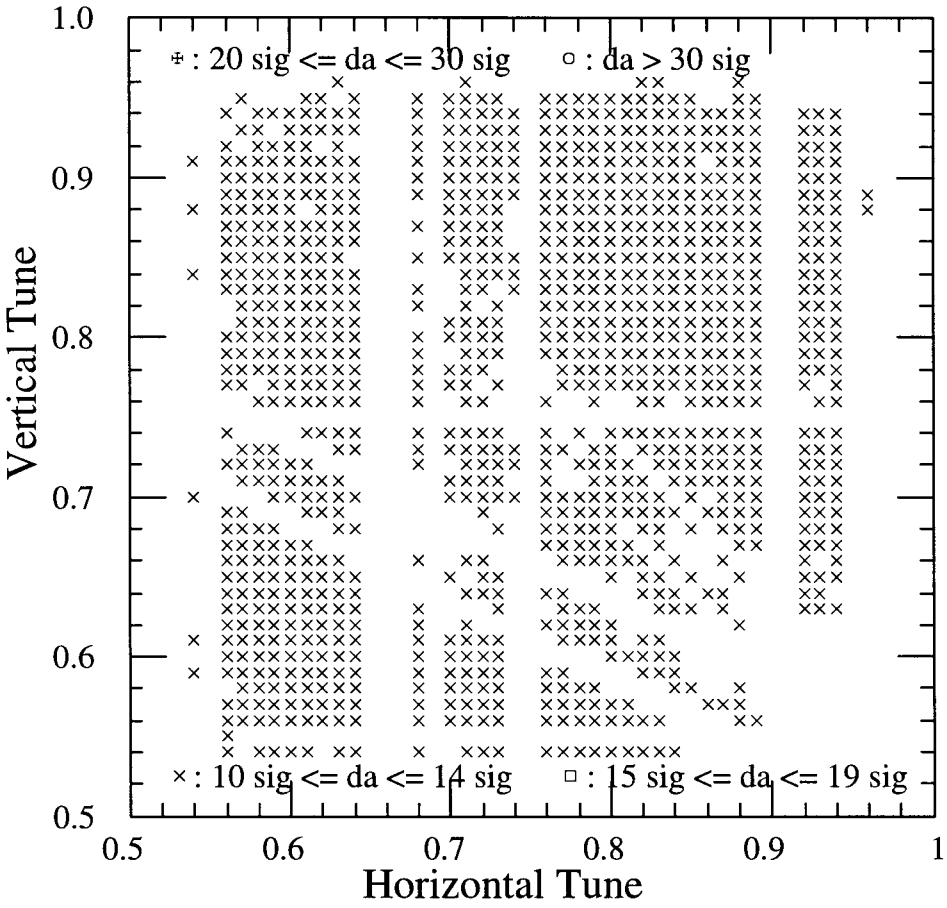

FIGURE 1: Dynamic aperture vs. tune point in the tune plane for a PEP-II High-Energy Ring with interlaced sextupoles, $\beta_y^* = 2cm$. Some resonance lines are clearly seen in the plot.

9 SWAMP PLOTS

Since the nPb tracking is very fast, one can easily get dynamic apertures for different working points throughout the tune plane by incrementing the working tunes μ_x and μ_y, while keeping all other terms in the resonance basis map fixed. This is equivalent to inserting an exactly matched linear trombone to switch the working tunes in the element-by-element tracking without further changing the lattice. We have generally found such swamp plots very informative. They have played an

essential role in evaluating and improving the PEP-II B-factory lattices. A typical PEP-II lattice swamp plots is shown in Fig. 1.

10 DIMENSIONLESS SCALING TRANSFORMATION

Up to this stage, the effective Hamiltonians, h_T, h_R, and the action coordinates, J_x, J_y, all have a dimension the same as the emittance while θ_x, θ_y, and δ arc dimensionless. Therefore it is very difficult to compare the coefficients, $C_{\vec{n}p}, A_{\vec{n}\vec{m}p}$, and $B_{\vec{n}\vec{m}p}$, among different orders since they would have different dimensions. In order to identify the key terms so as to probe their impact on the lattice nonlinear behavior, we would perform a scaling transformation such that

$$h_T = \epsilon_x \hat{h}_T, \qquad h_R = \epsilon_x \hat{h}_R, \qquad J_x = \epsilon_x \hat{J}_x, \qquad J_y = \epsilon_x \hat{J}_y,$$

where ϵ_x is the horizontal emittance, which in PEP-II is 48 nm-rad for the High-Energy Ring (HER) and 64 nm-rad for the the Low-Energy Ring (LER). Dropping the dimensionless symbol $\hat{}$, the dimensionless resonance basis map would be still given by Eq. 5, Eq. 6, Eq. 7, and Eq. 8 but each of the altered coefficients is now dimensionless.

11 TUNE SHIFT WITH AMPLITUDE

The effective Hamiltonian h_T given by Eq. 6 performs amplitude dependent rotations. The horizontal (x) and the vertical (y) tunes, as polynomial functions of the dimensionless invariants J_x and J_y and the dimensionless chromatic amplitude δ, can be calculated by the Hamilton's equations. They are given by

$$\nu_x(J_x, J_y, \delta) = \frac{1}{2\pi} \frac{\partial h_T(J_x, J_y, \delta)}{\partial J_x},$$

and

$$\nu_y(J_x, J_y, \delta) = \frac{1}{2\pi} \frac{\partial h_T(J_x, J_y, \delta)}{\partial J_y}.$$

To make fair comparisons of tune shift terms (and resonance terms – to be discussed) of different orders, we usually calculate the maximum of each term along the 10σ (10 times the nominal beam size) ellipse given by

$$r_x^2 + \frac{\epsilon_x}{\epsilon_y} r_y^2 = 10^2,$$

where $r_x = \sqrt{2J_x}$, and $r_y = \sqrt{2J_y}$ are radii in the two-dimensional phase-space planes. Note that we set $\epsilon_y = \frac{1}{2}\epsilon_x$ in consideration of a required vertical aperture that is sufficient for injection and for vertical blow-up from the beam-beam interaction.

In many occasions, we would also carry out the tune-shift-with-amplitude calculation using nonlinear normal forms in order to provide better accuracy.

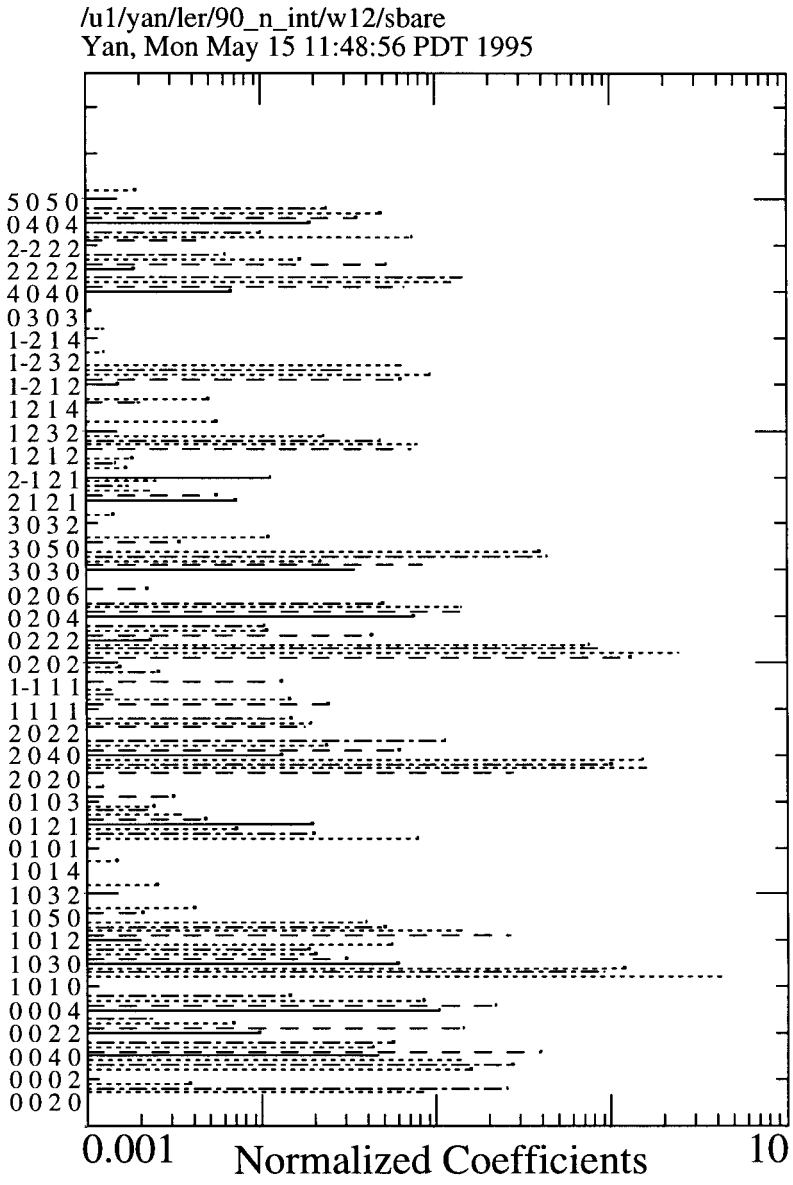

FIGURE 2: Normalized tune shift and resonance coefficients plotted in log scale horizontally. The vertical axis shows corresponding indices (m_x, m_y, n_x, n_y) for resonances and orders. The corresponding chromatic indices, p's, are not explicitly shown in the axis but are indicated with line patterns (p = 0: did, 1: dashes, 2: dots, 3: dotdashes, etc.

12 NORMALIZED RESONANCE BASIS COEFFICIENTS

The terms in the effective Hamiltonian h_R given by Eq. 7 and Eq. 8 perform angle- and amplitude-dependent nonlinear perturbations. These are the resonance driving terms. To fairly compare their driving strengths among different orders, we prefer to measure each of the phase-space step-sizes they would drive at a given turn, which is given by

$$|\Delta\vec{z}| = \sqrt{[(r_x\Delta\theta_x)^2 + (\Delta r_x)^2] + \frac{\epsilon_x}{\epsilon_y}[(r_y\Delta\theta_y)^2 + (\Delta r_y)^2]},$$

where $\Delta\theta_x, \Delta\theta_y, \Delta r_x,$ and Δr_y can be estimated for each term by taking its Poisson bracket with respect to the action-angle coordinates, $J_x, J_y, \theta_x, \theta_y$. Again, we would compute the maximum value of $|\Delta\vec{z}|$ for each term along the 10σ ellipse. $|\Delta\vec{z}| = 1$ means that the corresponding resonance can at most cause a phase-space motion of 1σ in one turn for a particle on the 10σ boundary. These maxima are what we call the normalized resonance basis coefficients. They can be plotted for a better identification of key terms as shown in Fig. 2 for an LER bare lattice.

13 SUMMARY

The mapping procedures described above have been frequently used for PEP-II lattice studies. By plotting the normalized resonance basis map coefficients, we can identify important tune shift and resonance terms that could degrade the dynamic aperture of the PER-II HER or LER lattices. We can confirm and understand their individual impacts on the dynamic aperture by modifying the global lattice and performing nPB tracking, and attempt to improve the lattices accordingly.

REFERENCES

1. A.J. Dragt, in *Physics of High-Energy Particle Accelerators*, AIP Conf. Proc. No. 87, edited by R.A. Carrigan et al. (AIP, New York, 1982);
2. M. Berz *Part. Accel.* **24** 109 (1989).
3. Y.T. Yan SSCL-500, in *Physics of Particle Accelerators*, AIP Conf. Proc. No. 249, edited by M. Month and M. Dienc (AIP, New York, 1982), p. 378; Y.T. Yan, SSCL-300 (1990).
4. J. Irwin, in this issue of *Particle Accelerators.*
5. E. Forest, M. Berz, and J. Irwin, *Part. Accel.* **24,** 91 (1989).
6. J. Irwin, in *Accelerator Physics at the SSC,* AIP Conf. Proc. No. 326, edited by Y.T. Yan et al. (AIP, New York, 1995), p. 662; D. Abell and A.J. Dragt, to be published.
7. J. Shi and Y.T. Yan *Phys. Rev. E,* **48,** 3943 (1993).
8. Y.T. Yan, et al. in *Proc. of Workshop on Nonlinear Problems in Future Particle Accelerators,* edited by W. Scandale and G. Turchetti (World Scientific, Singapore, 1990), p. 77.
9. R. Kleiss, F. Schmidt, and F. Zimmerman *Part. Accel.* **41,** 117 (1993).
10. Y.T. Yan, P. Channel, and M. Syphers *SSC Laboratory preprint* No. 157 (1993).
11. J. Irwin, N. Walker, and Y.T. Yan, SLAC-PUB-95-6779, in *Proc. of the 4th EPAC,* p. 899 *(1994).*
12. J. Irwin, T. Chen, and Y.T. Yan, SLAC-PUB-95-6727 (1995).
13. E. Courant and H. Snyder, *Ann. Phys.,* **3,** 1 (1958).